3.9.3

Neutron diffraction imaging at NOVA (J-PARC), HRPD, RESA, and TNRF (JRR-3)

Shin-ichi Shamoto[1], Tadashi Imaki[2], Hidetoshi Oshita[3,4], Takeshi Nakatani[3], Katsuaki Kodama[1], Naokatsu Kaneko[3,4], Hiroshi Suzuki[1], Hiroshi Iikura[1], Atsushi Moriai[1], Masahito Matsubayashi[1], Naoki Igawa[1], Kenji Yamaguchi[1], Kenji Masuko[2], Kensaku Sakamoto[2], Kentaro Suzuya[3], Toshiya Otomo[3,4]

[1]QuBS, Japan Atomic Energy Agency, Tokai, Ibaraki, 319-1195, Japan,

[2]Information Technology System's Management and Operating Office, Center for Computational Science & e-Systems, Tokai, Ibaraki, 319-1195, Japan,

[3]J-PARC Center, Japan Atomic Energy Agency, Tokai, Ibaraki, 319-1195, Japan,

[4]Institute of Materials Structure Science, High Energy Accelerator Research Organization (KEK), Tsukuba, Ibaraki, 305-0801, Japan

E-mail: shamoto.shinichi@jaea.go.jp

Abstract. Neutron diffraction imaging for a SUS430 plate (ϕ=25.0 mm, t=7.4 mm) embedded in a copper block sample (ϕ=50.0 mm and t=20.0 mm) has been tested at the high-intensity total diffractometer NOVA in J-PARC, the High-Resolution Powder Diffractometer HRPD and the diffractometer for Residual Stress Analysis RESA in JRR-3. The results are also compared with that measured at the Thermal Neutron Radiography Facility TNRF in JRR-3.

1. Introduction

The radiography is a technique to visualize inside of a material by radioactive ray transmission variation nondestructively. In the case of large metallic alloys such as bronze sculptures [1,2], a white neutron beam is very powerful because of the high transmittance and the high total flux. On the other hand, by using a monochromatic neutron beam, refraction contrast and ultra-small angle scattering property can be imaged, although the neutron flux is strongly reduced [3, 4]. Neutron phase imaging is a very sensitive method due to the refractive index contrast of a material. Polarized neutron imaging enables us to observe distribution of magnetic flux or magnetization of a material [5]. Neutron diffraction measurement is also a very powerful tool to observe crystal structure, lattice strain, phase ratio in a mixed sample, and so on. Its imaging can be a powerful tool to observe crystal structure distribution in a material. Energy-dispersive Bragg-edge imaging is one of the neutron diffraction imaging methods [2]. The other is a simple neutron diffraction imaging. As for x-ray diffraction imaging, heterogeneous materials were studied in a voxel size of 2.3×2.3×1.6 μm [6]. This small volume is achieved due to high intensity x-ray beam at synchrotron radiation facility (ESRF). In comparison with the synchrotron x-ray beam, neutron beam is still much weaker, but has a high

transmission capability. In addition, diffraction intensity of the highest intensity total diffractometer NOVA (BL-21) at the Materials and Life Science Facility (MLF) in J-PARC increases year by year [7]. We have checked the feasibility of diffraction imaging at various diffractometers, HRPD and RESA, at a continuous neutron source reactor, JRR-3 by measuring a test sample, a copper block with a SUS430 plate, in addition to at NOVA in J-PARC/MLF.

2. Experimental methods

The test sample composed of three pieces, as shown in Fig. 1. It was a copper block with a cylindrical cavity where a SUS430 plate was inserted. Copper atom has 11.81 barn in the total neutron cross section, while SUS430 with about 83 at% iron and about 17 % chromium has about 12.8 barn [8].

Neutron radiography was carried out at the Thermal Neutron Radiography Facility (TNRF) installed at 7R beam port in JRR-3 in Japan, where the average neutron flux was about 1.5 x 10^8 n/cm^2/sec. A radiography photo was taken for 4 sec. Neutron diffraction measurements were carried out at the Diffractometer for the Residual Stress Analysis (RESA) at T2-1 and the High Resolution Powder Diffractometer (HRPD) at 1G in JRR-3. The neutron fluxes for both diffractometers were about 1 x 10^5 n/cm^2/sec. The incident neutron wave lengths were 0.2073 nm and 0.1823 nm for RESA and HRPD, respectively. At the RESA, the sample was measured by $\Delta 2\theta$=0.1 deg. step with silts of W2 x H15 mm^2 before and after the sample for 100 and 220 sec at each step on copper and SUS430, respectively. At the HRPD, the sample was measured by 64 ^{3}He detectors with $\Delta 2\theta$=0.05 deg. step for 130 sec with a slit of W4 x H10 mm^2 only before the sample. The collimation was Open (35')-40'-Sample-6'.

Neutron diffraction imaging of the test sample was performed with 3x3 mm^2 resolution for about 4 days at high-intensity total diffractometer NOVA in J-PARC at 205-280 kW. The pulse peak neutron flux at the sample position of NOVA was about 1.0 x 10^7 n/cm^2/sec at 300 kW. For this measurement, the test sample is set on an aluminum rod fixed by a male screw of M4 on another copper bottom cap. So the aluminum rod has a female screw to fix it. A goniometer with 4 remote (*x, y, θ, RX*) and 1 manual (*RZ*) axes made by Meysho Kiko Co. was set at NOVA. Each measurement was carried out based on the neutron beam monitor count of NOVA (4.7M counts ~ 30 sec at 300 kW). Three natural sintered B_4C slits with 5 mm thickness were used to cut direct neutron beam to the sample, while the spectrometer slits were fully open. First one had a 20x20 mm^2 square hole. Second one narrowed the beam down to 3 mm vertically. Third one narrowed it down to 3 mm horizontally. The sample table on a goniometer was shifted horizontally and vertically by each 3 mm in 57x33 mm^2 (maximum 100x100 mm^2) normal to the beam. The sample table is rotated by 10 degrees step. Minimum scattered neutron transmission in this sample is 0.08% at λ=1.805 Å. Here we ignored this large neutron absorption in all cases for comparison. Diffraction data were taken only from left side of 90 degree banks (2θ=72~108 degrees) to the moderator of NOVA. In this configuration, Debye-Sherrer ring of a sample is covered by about 20%. In other words, diffracted intensity in the area is integrated, regardless of the crystallinity of the irradiated sample. Time in time of flight diffraction patterns was converted to *d*-value. Diffraction intensities in a specified *d*-range were mapped in an image as a photo by our original program "Neudift" [9], after subtracting the background automatically in addition to a simple absorption correction. The obtained photos were enlarged by MicroAVS.

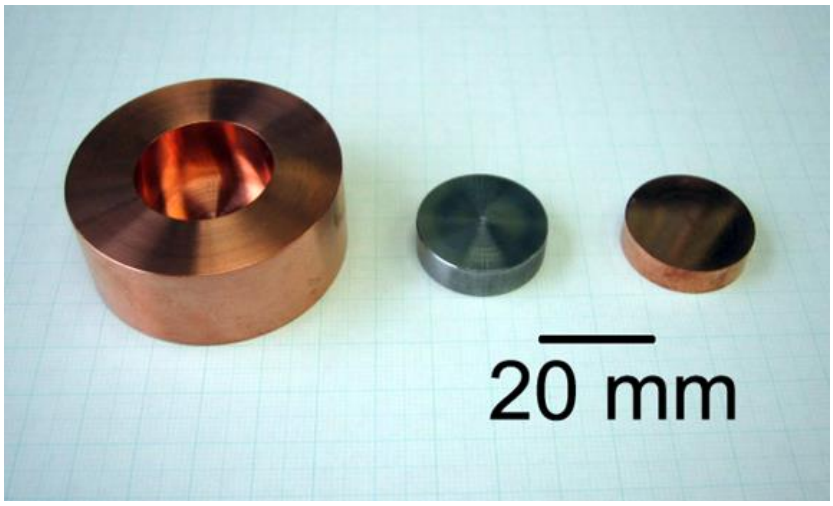

Figure 1. Used test sample pieces. From left, a copper block (ϕ=50.0 mm, t=20.0 mm) with a cylindrical cavity (ϕ=25.1 mm, d=14.5 mm), where a SUS430 plate (ϕ=25.0 mm, t=7.4 mm) was inserted, and capped by a copper plate (ϕ=25.0 mm, t=6.5 mm).

3. Results and Discussion

Figure 2 shows a side view of the test sample by neutron radiography measured at TNRF. The material difference between copper and SUS430 cannot be distinguished in the side view by the attenuation contrast regardless of the thickness. The opening gap with 0.6 mm width is weakly visible. This kind of difficulty can be overcome by using a diffraction technique, which is very sensitive to the structure. For example, copper has a face-centered cubic (FCC) structure with a lattice parameter of 3.6149 Å, while SUS430 has a body-centered cubic (BCC) structure with a=2.803 Å. Because of this structural difference, they were easily detected by the neutron diffraction patterns measured at HRPD, as shown in Fig. 3. Depending on the scattering area determined by incident and final neutron beams, the diffraction pattern changed drastically. At the reactor source, the neutron flux at the sample position is reduced by 3 orders of magnitudes, since only monochromatic neutron beam is used for the neutron diffraction. In this sense, the measuring time for the diffraction imaging may be increased by 3 orders of magnitudes.

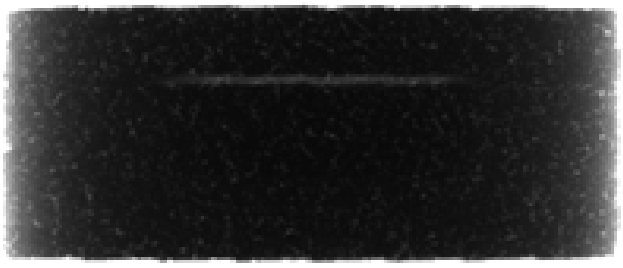

Figure 2. Radiography image for the packed sample of 3 pieces in Figure 1.

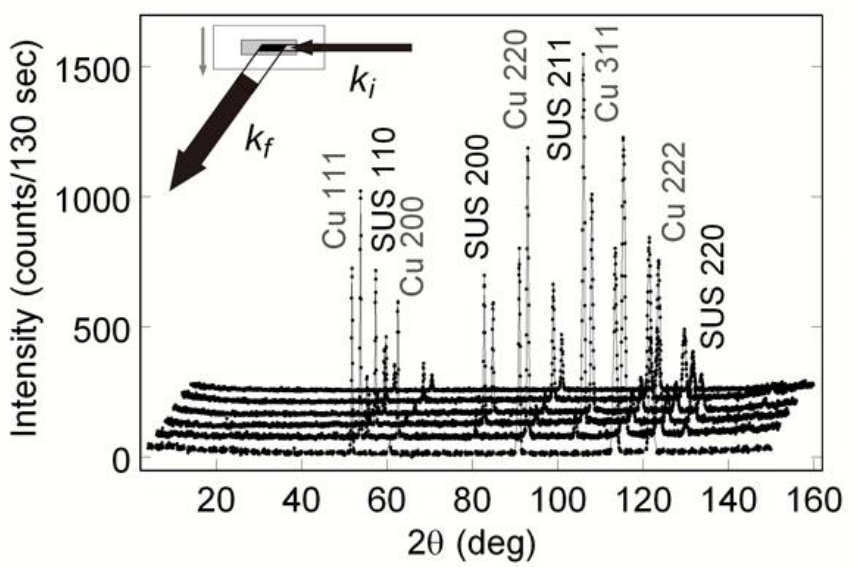

Figure 3. Neutron diffraction patterns of the test sample measured at HRPD from 1.5 mm to 21.5 mm by 4 mm step sliding along the gray axis in the inset. The diffraction pattern is shifted by 2 degrees and 50 counts each with increasing the sliding. Inset: Incident and final neutron wavevectors, k_i and k_f, are shown by black arrows with beam widths relative to the sample size. Positional scanning was carried out by sliding the black parallelogram scattering volume along the gray axis.

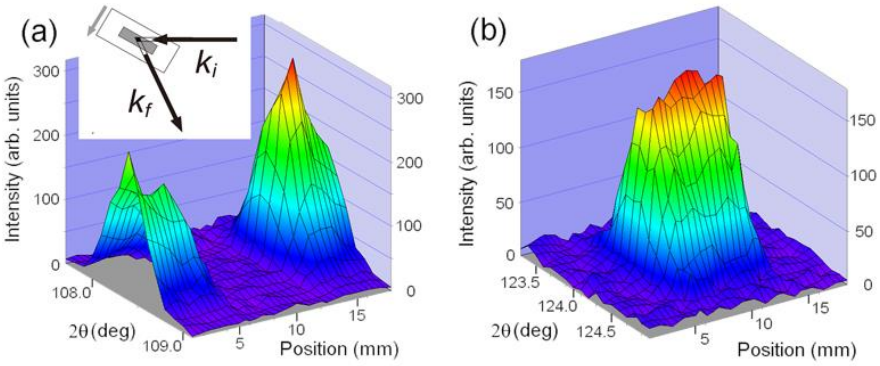

Figure 4. 3-dimentional neutron positional diffraction patterns of the test sample measured at RESA. The diffraction area was scanned by 0.5 or 1 mm step from 1 to 18 mm along the gray axis in the inset of (a). (a) 220 reflection for the FCC copper block. (b) 211 reflection for the BCC SUS430 plate. Inset: Incident and final neutron wavevectors, k_i and k_f, are shown by black arrows with beam widths relative to the sample size. Positional scanning was carried out by sliding the black parallelogram scattering volume along the gray axis.

Based on these results, we performed line structure scanning at RESA with narrow slits, which restricted the gauge volume as shown in the inset of Fig. 4(a). Two reflections of 220 for FCC copper and 211 for BCC SUS430 were measured at this diffractometer. The former reflection appeared at 2θ=108.4 degrees, while the latter peak was at 2θ=124.2 degrees as shown in Fig. 4. Since their

diffraction peaks have similar 2θ angles, the observed gauge volumes are the almost same to each other. The intensity weakly varies due to the possible large grain sizes of two materials. As shown in Fig. 4, the diffraction imaging clearly exhibited the positions of two materials, which contrasts to the photo in Fig. 2.

Figure 5 shows the side view of SUS430 plate in the copper block obtained by using high-intensity total diffractometer NOVA in J-PARC/MLF. The copper block and the aluminium rod weakly appear in the figure. Neutron absorption effect is corrected by a simple linear equation as a function of path length in the sample along x, which is normal to the direct beam direction z. This approximation corresponds to a limit of small absorption coefficient along x, but neglects the path along the incident beam. Event recording data were converted to d-dependent diffraction intensity table with an interval of Δd=0.01 Å. Integrated Bragg peak intensity at each pixel was obtained by simple summation of the intensities in the range of Δd=0.05 Å after subtracting both neighboring sides of diffraction intensities with the width of Δd=0.02 Å as a background. This intensity estimation method produces negative values on both sides of a positive peak due to the concave curve, which were regarded to be zero. Once 2D diffraction imaging is achieved, the tomography may be achieved with a set of various rotated data by using an existing tomography program.

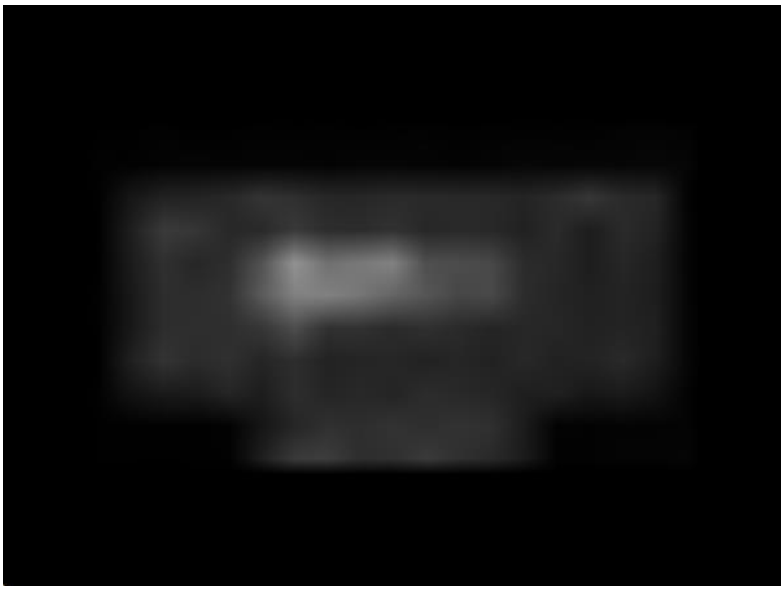

Figure 5. Neutron diffraction image of d~1.15 Å peak, corresponding to 211 reflection of the BCC SUS430 measured at NOVA.

Let us discuss the measuring efficiencies of diffraction imaging at various diffractometers. If we use slits with W x H before and T x H after the sample at the scattering angle 2θ, the measuring gauge volume V_g is $WHT/\sin 2\theta$. Here, we will define one Pixel Imaging Efficiency, PIE, which is defined simply to be Bragg peak intensity integrated by θ-2θ scan (counts/sec)/measuring time (sec)/gauge volume (mm^3).

In the experiment of RESA as shown in Fig. 4, V_g is 60-63 mm^3 depending on the scattering angle 2θ. Maximum integrated intensity of 220 reflection peak for the copper block with V_g of 63.2 mm^3 was 1448.1 counts/100 sec, while that of 211 reflection intensity for the SUS430 with V_g of 60.0 mm^3 was 1003.0 counts/100 sec. The background intensity was about 6-9 counts/100 sec. PIEs of RESA for copper 220 and SUS430 211 reflection peaks were 0.229 and 0.167, respectively.

As for the HRPD case with T=15 mm, maximum integrated intensity of 220 reflection peak for the copper block was 10426.2 counts/130 sec for V_g of 600.1 mm^3, while that of 211 reflection peak for the SUS430 was 4138.3 counts/130 sec for V_g of 613.4 mm^3. PIEs of HRPD for copper 220 and SUS430 211 reflection peaks were 0.134 and 0.052, respectively. The background intensity was about 23-39 counts/130 sec.

In the case of NOVA at J-PARC/MLF, maximum integrated intensity of 220 reflection peak for the copper block was 11646.8 counts/30 sec for V_g of 450 mm^3, while that of 211 reflection peak of the SUS430 was 772.3 counts/30 sec for V_g of 225 mm^3. PIEs of NOVA for copper 220 and SUS430 211 reflection peaks were 0.863 and 0.114, respectively. Under the long gauge volume conditions, these PIEs have large disadvantage of nearly one order of magnitude even in the former case in comparison with other diffractometers. Especially, in the latter case, the PIE value is strongly reduced due to the horizontal sample geometry. The background intensity was 30-44 counts/30 sec in these measurements.

As a result, all PIEs for these three diffractometers are comparable to each other for one measuring point at a d-value, although NOVA has several times higher efficiency than others. It should be noted that the multi-detector and time-of-flight instrument such as NOVA gives us a diffraction pattern in a wide Q-range all at once. This can further extend additional efficiency of wide-Q range measurement, resulting in an important merit even in comparison with that of high-intensity synchrotron x-ray diffractometers.

For a diffractomer monochromated by highly ordered pyrolytic graphite, the incident neutron flux is strongly reduced from the white neutron beam. Alternative way to get high intensity would be to use broad neutron spectrum at the sacrifice of the Q-resolution in the diffraction measurement to specialize the diffractometer for the diffraction imaging.

Here, we showed the efficiency of neutron diffraction imaging at various diffractometers. By using multi-detector system, the efficiency for a wide-Q range measurement can be dramatically improved even at the same diffractometer. Neutron lens can also increase the efficiency. In addition to the reciprocal space measurement, we may measure the atomic pair distribution function (PDF), in other word, real space measurement analysis, in the small area, which enables us to study phase separation, decomposition of amorphous or inhomogeneous liquid materials, for example.

Anyway, these nondestructive analyses would be very helpful for studying the inside of industrial materials with many phases. Among the various quantum beams, the neutron is a unique beam for the high penetration and the high sensitivity for light elements and magnetic moments. Intense pulse neutron sources such as J-PARC/MLF may provide us a chance to explore new type of imaging fields. In our previous study, crystal structures in an ammonite fossil were studied as an example by the neutron diffraction imaging method at NOVA in J-PARC [10].

4. Summary

The measuring efficiencies of diffraction imaging at various diffractometers are studied by using a simple test sample. Obtained efficiencies were comparable to each other for one measuring point. But time-of-flight measurement can multiply the efficiency significantly due to the time-of-flight method with a wide Q-range. Existing diffractometers such as RESA can be used for this scanning down to the sub-mm resolution. In order to reduce the diffraction volume, multi-detectors, neutron optics, and special monochromator with low Q-resolution are to be equipped. In addition, high intensity neutron source is inevitable. Possible new fields to be explored by this diffraction imaging were also discussed.

Acknowledgments

The authors would like to thank Drs. H. Matsue, T. Taguchi, A. Hoshikawa, Y. Ishii, M. Kureta, M. Segawa, and S. Iikubo for their help and fruitful discussions. This work was benefited from the use of following instruments, NOVA at J-PARC (Proposals 2012B0172, 2013B0099), RESA, HRPD, and TNRF at JRR-3.

References

[1] E. H. Lehmann, Neutron News, **17**-1, 22 (2006).
[2] "Neutron Imaging and Applications: A Reference for the Imaging Community" (Springer, 2009): Ian S. Anderson, Robert L. McGreevy and Hassina Z. Bilheux.
[3] W. Treimer, M. Strobl, A. Hilger, C. Seifert, and U. Feye-Treimer, Appl. Phys. Lett. **83**, 398 (2003).
[4] M. Strobl, W. Treimer, and A. Hilger, Appl. Phys. Lett., **85**, 19 (2004).
[5] N. Kardjilov, I. Manke, M. Strobl, A. Hilger, W. Treimer, M. Meissner, T. Krist and J. Banhart, Nature Phys. **4** (2008) 399.
[6] P. Bleuet, E. Welcomme, E. Dooryhee, J. Susini, J.-L. Hodeau and P. Walter, Nature Mat. **7** (2008) 468.
[7] H. Ohshita, T. Otomo, S. Uno, K. Ikeda, T. Uchida, N. Kaneko, T. Koike, M. Shoji, K. Suzuya, T. Seya and M. Tsubota, Nucl. Instrum. Methods Phys. Res. Sect. A **672** (2012) 75.
[8] Albert-Jose Dianoux, and Gerry Lander, *Neutron Data Booklet* (Institute Laue-Langevin, Grenoble, 2002).
[9] Diffraction intensity mapping program "Neudift" ver. 1 is developed by one of the authors, Mr. Tadashi Imaki, for conversion of diffraction data sets to a photo.
[10] Shin-ichi Shamoto, Katsuaki Kodama, Tadashi Imaki, Takeshi Nakatani, Hidetoshi Oshita, Naokatsu Kaneko, Kenji Masuko, Kensaku Sakamoto, Kenji Yamaguchi, Kentaro Suzuya, Toshiya Otomo, JPS Conf. Proc. 1, 014011 (2014)